Clinical Cancer Research

A Vaccinia Virus Armed with Interleukin-10 Is a Promising Therapeutic Agent for Treatment of Murine Pancreatic Cancer

Louisa S. Chard[1], Eleni Maniati[2], Pengju Wang[3], Zhongxian Zhang[3], Dongling Gao[3], Jiwei Wang[3], Fengyu Cao[3], Jahangir Ahmed[1], Margueritte El Khouri[1], Jonathan Hughes[1], Shengdian Wang[4], Xiaozhu Li[4], Bela Denes[5], Istvan Fodor[5], Thorsten Hagemann[2], Nicholas R. Lemoine[1,3], and Yaohe Wang[1,3]

Abstract

Purpose: Vaccinia virus has strong potential as a novel therapeutic agent for treatment of pancreatic cancer. We investigated whether arming vaccinia virus with interleukin-10 (IL10) could enhance the antitumor efficacy with the view that IL10 might dampen the host immunity to the virus, increasing viral persistence, thus maximizing the oncolytic effect and antitumor immunity associated with vaccinia virus.

Experimental Design: The antitumor efficacy of IL10-armed vaccinia virus (VVLΔTK-IL10) and control VVΔTK was assessed in pancreatic cancer cell lines, mice bearing subcutaneous pancreatic cancer tumors and a pancreatic cancer transgenic mouse model. Viral persistence within the tumors was examined and immune depletion experiments as well as immunophenotyping of splenocytes were carried out to dissect the functional mechanisms associated with the viral efficacy.

Results: Compared with unarmed VVLΔTK, VVLΔTK-IL10 had a similar level of cytotoxicity and replication *in vitro* in murine pancreatic cancer cell lines, but rendered a superior antitumor efficacy in the subcutaneous pancreatic cancer model and a K-ras-p53 mutant-transgenic pancreatic cancer model after systemic delivery, with induction of long-term antitumor immunity. The antitumor efficacy of VVLΔTK-IL10 was dependent on $CD4^+$ and $CD8^+$, but not NK cells. Clearance of VVLΔTK-IL10 was reduced at early time points compared with the control virus. Treatment with VVLΔTK-IL10 resulted in a reduction in virus-specific, but not tumor-specific $CD8^+$ cells compared with VVLΔTK.

Conclusions: These results suggest that VVLΔTK-IL10 has strong potential as an antitumor therapeutic for pancreatic cancer.
Clin Cancer Res; 21(2); 405–16. ©2014 AACR.

Introduction

Pancreatic cancer is the fourth leading cause of cancer-related death worldwide (1) and remains consistently lethal with a 5-year survival rate of less than 5%. This situation signifies a need for radically new therapeutic strategies that are not subject to cross-resistance with conventional therapies.

Oncolytic viruses have emerged as attractive therapeutic candidates for cancer treatment due to their inherent ability to specifically target and lyse tumor cells and induce antitumor effects. An engineered replication-competent Adenovirus, *dl1520* (ONYX-015), was the first of these viruses to be tested for human pancreatic cancer treatment. The treatments were well tolerated, but no objective responses with virus therapy alone were seen in any of the patients (2).

Vaccina virus has strong potential for exploitation as both an oncolytic agent and vector for therapeutic gene delivery to tumors. Extremely promising clinical trial data have recently emerged in which GM-CSF–armed vaccinia virus induced objective responses in patients with liver, colon, kidney, and lung cancer and melanoma (3, 4). Vaccinia virus has several inherent features that make it particularly suitable for use as an oncolytic agent, including fast and efficient replication with rapid cell-to-cell spread, natural tropism for tumors, a well-documented safety record, and an ability to replicate in many different cell types, a feature not shared by adenoviruses. We recently demonstrated that hypoxia, which contributes to the aggressive and treatment-resistant phenotype of pancreatic ductal adenocarcinoma (PDAC; ref. 5), does not inhibit and may even enhance the potency of oncolytic vaccinia virus (6). In addition, vaccinia virus has recently been shown to be effective at human tumor targeting after intravenous delivery (4).

Interleukin-10 (IL10), first described as a factor produced by Th2 clones capable of inhibiting Th1 cytokine production (7), is a potent inhibitor of T cell–mediated antiviral responses by prevention of dendritic cell (DC) activation of the $CD4^+$Th1 inflammatory pathway (8, 9). IL10 is a key player in the establishment

[1]Center for Molecular Oncology, Barts Cancer Institute, Queen Mary University of London, London, United Kingdom. [2]Center for Cancer and Inflammation, Barts Cancer Institute, Queen Mary University of London, London, United Kingdom. [3]Sino-British Research Centre for Molecular Oncology, Zhengzhou University, Zhengzhou, China. [4]CAS Key Laboratory of Infection and Immunity, Institute of Biophysics, Chinese Academy of Sciences, Beijing, China. [5]Center for Health Disparities and Molecular Medicine, Loma Linda University, Loma Linda, California.

Note: Supplementary data for this article are available at Clinical Cancer Research Online (http://clincancerres.aacrjournals.org/).

Corresponding Authors: Yaohe Wang, Centre for Molecular Oncology, Barts Cancer Institute, Queen Mary University of London, London EC1M 6BQ, United Kingdom. Phone: 44-207-8823596; Fax: 44-207-8823884; E-mail: Yaohe.wang@qmul.ac.uk; and Nick Lemoine, bci-director@qmul.ac.uk

doi: 10.1158/1078-0432.CCR-14-0464

Translational Relevance

Oncolytic virotherapy is beginning to show promise as a realistic alternative to standard cancer therapeutics. To date, clinical trials have proved this strategy safe and well tolerated by patients; however, clinical responses after treatment with virus alone have been modest. A new generation of oncolytic viruses that engage the host immune system in the attack against the tumor are providing more encouraging clinical results. This study demonstrates that vaccinia virus armed with the cytokine interleukin-10 (IL10) is a novel and extremely promising therapeutic for treatment of pancreatic tumors and prevention of disease recurrence. Understanding the mechanisms by which IL10 improves oncolytic virotherapy provides a foundation for the rational design of clinical trials for treatment of pancreatic cancer and other solid tumors with this virus and provides valuable information for the design of future antitumor strategies that aim to combine oncolytic virotherapy with immunotherapeutic approaches.

and perpetuation of viral persistence *in vivo* (10, 11). Therefore, arming vaccinia virus with IL10 may prolong viral persistence and enhance the antitumor efficacy. IL10 has historically been regarded as an immunosuppressive cytokine that has extensively been described in association with cancer, including pancreatic cancer (12, 13), as a mechanism of tumor escape from immunosurveillance (14, 15). However, accumulating evidence demonstrates that IL10 also has immunostimulatory and antitumor properties (16). Functional mechanisms investigated include activation of natural killer (NK) cells (17) that have been associated with tumor clearance in murine models of breast and colorectal cancer (18); inhibition of angiogenesis; enhancement of macrophage infiltration into tumors (19); and prevention of metastasis by inhibition of matrix metalloproteinase-2 (20). A number of preclinical (21) and clinical trials have consistently demonstrated safety of IL10 administration in treatment of diseases, including psoriasis (22), Crohn disease (23), and chronic hepatitis C infection (24), which make a strong case for its use as a therapeutic modality in cancer. IL10 has been reported to enhance the therapeutic effectiveness of a vaccinia virus–based vaccine against murine cancer cells (25), which may be connected to its ability to enhance the growth and proliferation of T cells (26) or its role as a chemotactic agent for $CD8^+$ T cells. Unfortunately, the half-life of IL10 is only approximately 20 minutes and it is difficult to maintain a high concentration after administration of recombinant protein (27). Nonreplicating adenovirus-mediated delivery has shown promise in retaining therapeutically effective levels of IL10 *in vivo* (28). Given its pleiotropic effects, IL10 may be an effective agent with which to improve the antitumor potential of vaccinia virus.

In this study, we have tested a Lister strain, TK-deleted replicating vaccinia virus armed with murine IL10 (VVLΔTK-IL10) in subcutaneous and transgenic murine models of pancreatic cancer and demonstrated that VVLΔTK-IL10 has far superior antitumor activity compared with unarmed vaccinia virus (VVLΔTK), resulting in almost complete tumor clearance, significantly increased survival times, and the production of long-term tumor immunity in the host. Our results suggest that VVLΔTK-IL10 has strong potential as an effective treatment for pancreatic cancer and lays the foundation for translation of this therapeutic into a clinical setting.

Materials and Methods

Cell lines and viruses

The murine PDAC cell line DT6606 and the preinvasive pancreatic cancer (PanIN) cell line DT4994 were cultured from LSL-$Kras^{G12D/+}$;Pdx-1-Cre mice that had developed PDAC (29). These were kindly provided by David Tuveson (Cancer Research UK Cambridge Research Institute, Cambridge, United Kingdom; now at Cold Spring Harbor Laboratory). The DT6606-ovalbumin (OVA) stable cell line was created by transfection of DT6606 cells at with pCI-neo-cOVA (Addgene) using Effectene transfection reagent (Qiagen) according to the manufacturers' protocol. CV1 (African monkey kidney) cells and PT45 (human pancreatic carcinoma) cells were obtained from the American Type Culture Collection (ATCC).

Construction and production of recombinant vaccinia virus Lister strains VVLΔTK-IL10 (rVV-IL10, armed with murine IL10) and VVLΔTK (rVV-L15) were previously described (30, 31).

Vaccinia virus replication assay

Appropriate cell lines were seeded in triplicate and infected 16 hours later with VVLΔTK or VVLΔTK-IL10 at a multiplicity of infection (MOI) of 1 plaque-forming unit (PFU) per cell. Cells and supernatant were collected at 24, 48, and 72 hours after infection and titers were determined by measuring the median tissue culture infective dose ($TCID_{50}$) on indicator CV1 cells. The Reed–Muench mathematical method was used to calculate the $TCID_{50}$ value for each sample (32). Viral burst titers were converted to PFU per cell based on the number of cells present at viral infection. One-way ANOVA followed by Bonferroni post-test was used to assess significance.

Cell cytotoxicity assay

The cytotoxicity of the viruses in each cell line was assessed 6 days after infection with virus using an MTS nonradioactive cell proliferation assay kit (Promega) according to the manufacturer's instructions, which allowed determination of an EC_{50} value (dose required to kill 50% of cells).

Real-time quantitative PCR

Subcutaneous tumors collected from treated mice were homogenized before DNA was extracted using the QIAamp DNA Blood Mini Kit (Qiagen Ltd.) according to the manufacturer's instructions. TaqMan system primers and probes (Supplementary Table S1) were designed using Primer Express v3.0 software (Applied Biosystems) and constructed by Sigma-Aldrich and Applied Biosystems, respectively. Samples, controls, and standards were tested in triplicate by quantitative polymerase chain reaction (qPCR) using 7500 Real-time PCR System. Results were normalized to NanoDrop readings and expressed as genome copy number/0.01 g tumor tissue. One-way ANOVA followed by Bonferroni post-test was used to assess significance.

IL10 and interferon-γ ELISA

IL10 or interferon-γ (IFNγ) protein levels were quantified using an IL10-specific or IFNγ-specific ELISA (R&D Systems) according to the manufacturer's instructions. Where appropriate, data were normalized to cell number present at time of infection.

Splenocyte preparation

Spleens were extracted from mice, combined with complete T-cell medium (RPMI medium, 10% BCS, 1% penicillin–streptomycin, and 1% sodium pyruvate), and cells were separated using a 70-μm cell strainer. Cells were resuspended in red blood cell lysis buffer (Sigma-Aldrich), washed in PBS, and the pellet was resuspended in T-cell medium.

***In vitro* splenocyte restimulation**

Cells (2×10^6) were aliquotted into each well of a 96-well plate in duplicate. Cells were restimulated with either a vaccinia virus–specific B8R peptide (TSYKFESV; Proimmune) at a final concentration of 20 μg/mL or 5×10^5 mitomycin C–treated DT6606-OVA cells. Restimulated splenocytes were incubated at 37°C/5% CO_2 for 72 hours and the supernatant was collected.

Tumor cell preparation

Tumor cell suspensions were prepared by incubation with 1× collagenase/hyaluronidase (STEMCELL TECHNOLOGIES) for 30 minutes at 37°C. Cells were separated using a 70-μm cell strainer and resuspended in complete T-cell medium.

Immunophenotyping of splenocytes and tumors

All fluorochrome-conjugated antibodies were supplied by eBiosciences and used at a 1:200 dilution. The B8R and OVA H-2Kb-restricted, MHC class I pentamers were synthesized by Proimmune and used at a 1:20 dilution.

Splenocytes and tumors were prepared and aliquotted into 96-well U-bottom plates. Pentamer staining was carried out by resuspending cells in FACS buffer (FB; PBS+1% heat-inactivated BCS+0.1%NaN_3) plus pentamer and incubating at room temperature for 10 minutes. Cells were washed before being incubated in FB plus appropriate fluorescent marker-conjugated anti-immune cell marker antibodies for 30 minutes on ice. Cells were washed and fixed in 2% formalin before analysis using a BD LSR Fortessa flow cytometer. Data were analyzed using FlowJo software (TreeStar Inc).

***In vivo* studies**

All animal studies were carried out under the terms of the Home Office Project Licence PPL 70/6030 and subject to Queen Mary University of London ethical review, according to the guidelines for the welfare and use of animals in cancer research (33).

The C57/BL6 mouse is H-2 haplotype-identical to the injected DT6606 cells thus DT6606 allografts could be established in the right flank of 3- to 4-week male C57/BL6 mice by injecting 3×10^6 DT6606 cells. When tumors reached around 0.6 cm in diameter, mice were stratified by tumor size into groups of 8 and received 100-μL intratumoral (i.t.) injections of 1×10^8 PFU of VVLΔTK, VVLΔTK-IL10, or PBS daily for 5 days. Tumor size was measured twice weekly until the death of the first animal in each group and volume was estimated [volume = (length × width^2 × π)/6]. Survival analysis was carried out using the Kaplan–Meier survival curves with log-rank (Mantel–Cox) tests used to assess significance. Mice that had cleared tumor after treatment were rechallenged 4 weeks after clearance in the opposite flank with 4×10^6 DT6606 cells and tumor volume was estimated as previously. For immune depletion studies, DT6606 subcutaneous tumors were established as described and 1 day before commencement of viral treatment 200 μg of anti-CD4 IgG (antibody clone GK1.5), anti-CD8 IgG (antibody clone TIB210), anti-NK IgG (antibody clone PK136), or control rat IgG was injected intraperitoneally (i.p.) in 200-μL PBS. Injections were continued twice weekly for the duration of the experiment and FACS analysis was used to verify depletion for the duration of the experiment. Five mice per group were treated and the experiment was carried out twice.

Transgenic mice

LSL-Kras$^{G12D/+}$;LSL-Trp53$^{R172H/+}$;Pdx-1-Cre (KPC) mice were kindly provided by David Tuveson (Cancer Research UK Cambridge Research Institute) and have been described previously (29). Mice were treated when they reached 2.5 months, previously demonstrated to be the mean age at which PanINhas progressed to PDAC (29). Mice were treated i.p. with 2×10^8 PFU/injection VVLΔTK or VVLΔTK-IL10 on days 1, 3, and 5. Mice were examined daily for signs of disease progression and culled when they showed symptoms of sickness. Survival data were compared using Prism (GraphPad Software) and a log-rank (Mantel Cox) test was used to determine significance of survival differences.

***In vivo* imaging**

Seven days after treatment of KPC or KP mice, the biodistribution of VVLΔTK was determined in anesthetized animals (2% isofluorane inhalation) after i.p. injection of D-luciferin (150 mg/kg; Xenogen) and fluorescence measured with the IVIS camera (Xenogen Corp.).

Histopathologic examination and immunohistochemistry for viral proteins

KPC or control KP mice (2.5-month old) were treated i.p. with 2×10^8 PFU/injection VVLΔTK or VVLΔTK-IL10 on days 1, 3, and 5. On relevant days, animals were sacrificed, the pancreas removed, snap-frozen, and stored at −80°C. Frozen tissue was processed for immunohistochemistry (IHC) analysis of vaccinia virus coat protein [1:50 rabbit anti-vaccinia virus coat protein polyclonal antibody (MorphoSys UK Ltd.)], macrophage [1:2,000 anti-F4/80 antibody (Serotech)], $CD3^+$ T cell [1:200 anti-CD3 antibody (BioLegend)], or $CD8^+$ T cell [1:300 anti-CD8 antibody (BioLegend)] as described previously (31).

Results

VVLΔTK-IL10 replicates efficiently *in vitro* in murine cancer cell lines derived from a transgenic mouse model of pancreatic cancer

To determine whether inclusion of IL10 affected on characteristics of VVLΔTK *in vitro*, replication and cytotoxicity in three cell lines were examined; DT6606, representing late-stage invasive PDAC and DT4994, representing PanIN, were both derived from the K-ras transgenic mouse model of pancreatic cancer (29). DT6606-OVA, in which the OVA antigen is overexpressed in DT6606 cells, was also examined. All cell lines supported production of infectious virions of VVLΔTK and VVLΔTK-IL10 (Fig. 1A–C) and IL10 did not act to inhibit nor promote viral replication. The EC_{50} was comparable between VVLΔTK and VVLΔTK-IL10 (Fig. 1D). Furthermore, IL10 was expressed in all three cell lines over 72 hours after infection (Fig. 1E). Thus, arming VVLΔTK with IL10 does not adversely affect the *in vitro* oncolytic effect desired for our virotherapy strategy.

VVLΔTK-IL10 infection was also assessed in the human pancreatic cancer cell line PT45 to demonstrate potential translation

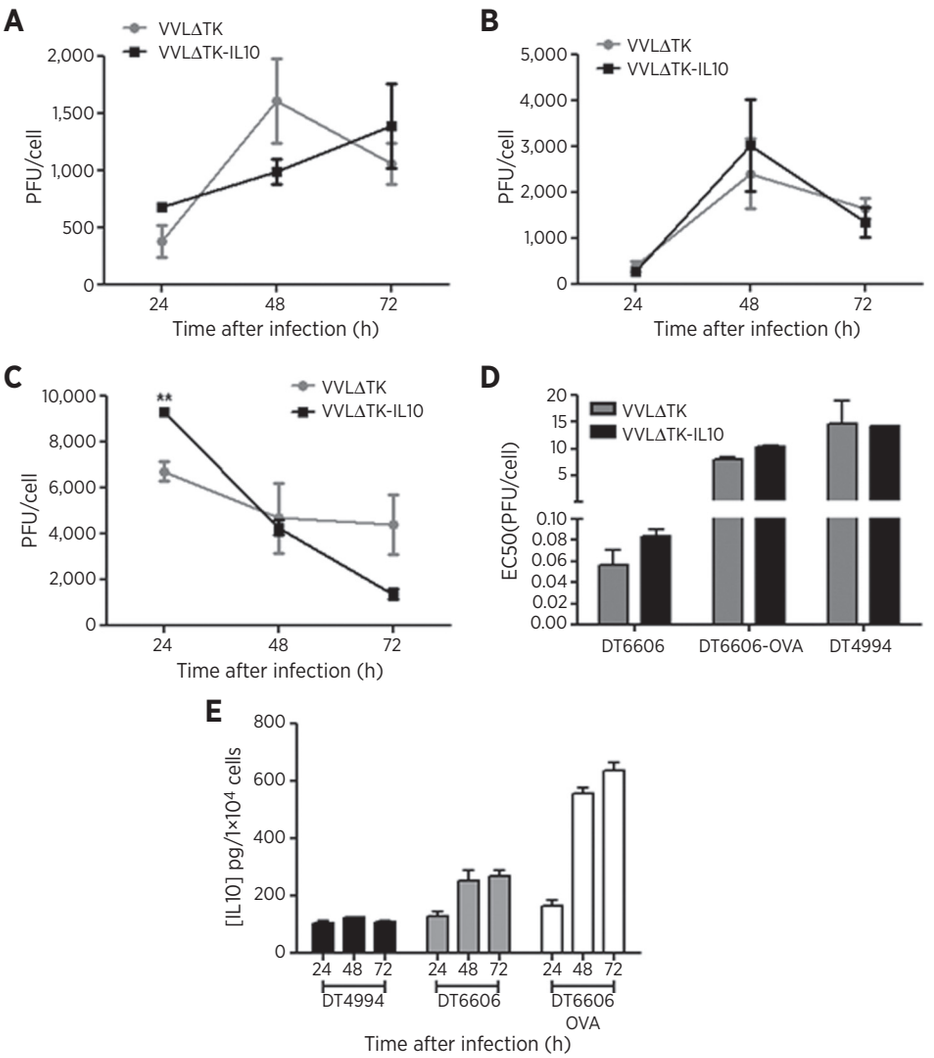

Figure 1.
Replication, potency, and protein expression of IL10 by VVLΔTK and VVLΔTK-IL10 *in vitro*. A–C, production of infectious virions in murine DT6606 (A), DT6606-0VA (B), and DT4994 (C) cells. Mean viral replication ± SEM was determined by $TCID_{50}$ assay on CV1 cells. Statistical analysis was carried out using a Students unpaired *t* test at each time point. **, $P < 0.01$. D, cytotoxicity of VVLΔTK and VVLΔTK-IL10 against DT6606, DT6606-OVA, and DT4994 cells. Cell death was determined by the MTS assay 144 hours after infection. Mean EC_{50} values ± SEM are shown. E, expression of IL10 by VVLΔTK-IL10. Cells were infected with VVLΔTK-IL10 at an MOI of 1 PFU/cell. Supernatant was collected every 24 hours for 72 hours and assayed for IL10 by ELISA. Data were normalized to cell number infected and are displayed as pg IL10/1 × 10^4 cells.

of this therapy into human cells. VVΔTK-IL10 showed efficient replication, cytotoxicity, and IL10 expression in this cell line (Supplementary Fig. S1).

VVLΔTK-IL10 shows superior antitumor efficacy compared with VVLΔTK in immunocompetent mouse models of pancreatic cancer

In vivo efficacy of VVLΔTK-IL10 was examined using a subcutaneously established pancreatic cancer model. DT6606 subcutaneous tumors were established in male C57/BL6 mice and the animals received i.t. injections of 1 × 10^8 PFU of VVLΔTK, VVLΔTK-IL10, or PBS daily for 5 days. The selected viral dose was 10 times lower than the most commonly reported 1 × 10^9 PFU/dose in the literature (34). Both VVLΔTK and VVLΔTK-IL10 demonstrated antitumor efficacy (Fig. 2A). However, treatment with VVLΔTK-IL10 resulted in a superior antitumor efficacy by day 44, with 87.5% of mice showing tumor clearance and significantly improved overall survival rates compared with both VVLΔTK- and PBS-treated animals (Fig. 2B). The C57/Black6 mouse is H-2 haplotype-identical to the injected DT6606 cells. Growth of tumors in PBS-treated animals confirmed that there was no immunologic rejection of the DT6606 cell line due to MHC or minor antigen mismatches.

To determine whether VVLΔTK-IL10 remained efficacious in a more pathologically relevant model of pancreatic cancer, KPC transgenic mice were used. In these mice, pancreas-specific expression of mutant $Kras^{G12D}$ and $Trp53^{R172H}$ results in progressive development of PDAC (35). Three doses of virus (2 × 10^8 PFU/day) were given i.p. to 2.5-month old, PDAC-bearing mice. To confirm the specificity of virus for pancreatic tumors after i.p. injection, VVLΔTK, which expresses a luciferase transgene in the viral TK region, was injected into either experimental KPC mice or control KP mice. Two days later, mice were imaged for luciferase expression (Fig. 2C). Strong luciferase signals were obtained specifically in the pancreatic area of KPC transgenic mice (Fig. 2C, left), while no signal was obtained from control mice (Fig. 2C, right). The vaccinia virus proteins were expressed in cancer cells and proliferative acinar cells in KPC mice (Fig. 2C, left, bottom), whereas no viral protein expression was observed in the ductal epithelial cells and acinar cells in KP mice (Fig. 2C, right, bottom), confirming

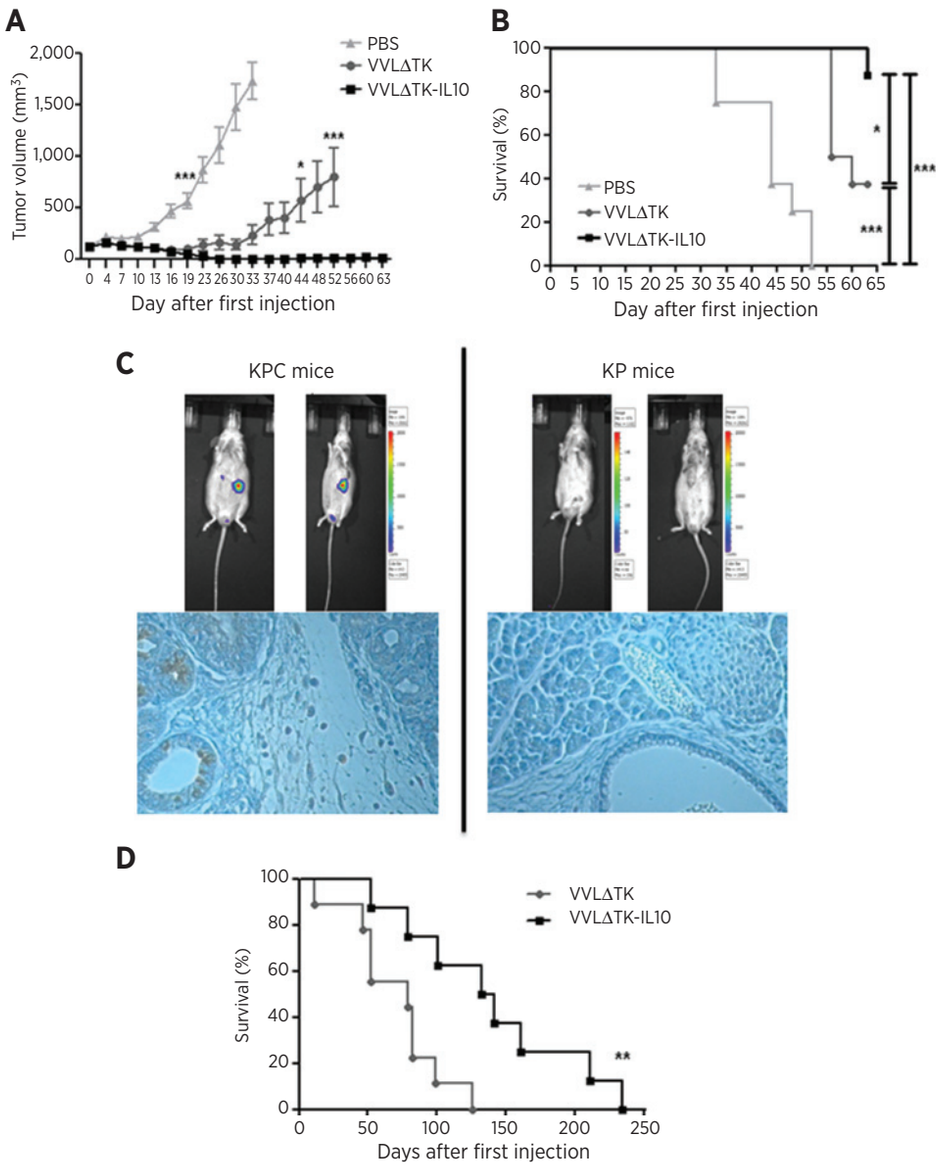

Figure 2.
Efficacy of VVLΔTK and VVLΔTK-IL10 against pancreatic tumors *in vivo*. DT6606 cells were injected into the right flank of male C57/Black6 mice. Eight mice/group were injected i.t. with 1×10^8 PFU VVLΔTK, VVLΔTK-IL10, or PBS daily for 5 days. Mean tumor size ± SEM are displayed until the death of the first mouse in each group and compared by one-way ANOVA with *post hoc* Bonferroni testing. A, tumor growth curve of DT6606 tumors treated by i.t. injection. Both treatments significantly reduce tumor growth compared with PBS at day 19 (***, $P < 0.001$) and VVLΔTK-IL10 significantly reduces tumor growth compared with VVLΔTK by day 44 (*, $P < 0.05$; ***, $P < 0.001$). B, the Kaplan–Meier survival analysis of mice bearing DT6606 tumors after i.t. treatment. The log-rank (Mantel–Cox) tests indicate that both treatments significantly improve survival compared with PBS ($P < 0.0001$). *, $P = 0.03$ (VVLΔTK vs. VVLΔTK-IL10). C, 2.5-month-old KPC (LSL-Kras $G12D^{+/-}$;LSL-$p53R172H^{+/-}$;Pdx-1-Cre; left) or KP (LSL-Kras $G12D^{+/-}$;LSL-$p53R172H^{+/-}$;Cre^{-}), which do not express Cre (right) transgenic mice were injected i.p. with 2×10^8 PFU/mL VVKΔTK on days 1, 3, and 5. On day 7, mice were imaged using the IVIS imaging system ($n = 2$/group). Pancreatic tissue was also harvested for each mouse, sectioned, IHC staining was performed for detection of vaccinia virus coat protein (brown), which colocalized within tumor cells in the pancreas of KPC mice but was absent from KP mice. D, the Kaplan–Meier survival analysis of KPC transgenic mice ($n = 10$/group) injected i.p. with 2×10^8 PFU VVLΔTK or VVLΔTK-IL10 on days 1, 3, and 5 after the animals reached 2.5 months. Significance was assessed using the log-rank (Mantel–Cox) tests. *, $P < 0.05$; **, $P < 0.01$.

specificity of replication of TK-deleted vaccinia virus for pancreatic tumor cells. Efficacy of viral treatment in this model was assessed by survival (Fig. 2D). Treatment with VVLΔTK-IL10 resulted in significantly improved survival rates compared with treatment with VVLΔTK. Mean survival time for VVLΔTK-IL10–treated animals after commencement of treatment was 138.5 days compared with 69.7 days for VVLΔTK–treated animals, suggesting VVLΔTK-IL10 as an extremely effective treatment for PDACs even in the most complex murine models of the disease.

Treatment with VVLΔTK-IL10 results in long-term protection against disease recurrence

Successful OV strategies aim not only to eradicate the primary tumor, but also to induce long-term antitumor immunity to prevent disease recurrence. Thus, animals were rechallenged with 4×10^6 DT6606 cells 4 weeks after complete regression of the primary tumor (Fig. 3A). Treatment with both viruses resulted in long-term immunity to DT6606 tumor cells as evidenced by rapid clearance of these cells that necessitated no further viral treatments. Interestingly, VVLΔTK-IL10–treated animals were able to clear the secondary tumor more quickly and more consistently than VVLΔTK-treated animals.

$CD8^+$ and $CD4^+$, but not NK cells, are required for VVLΔTK-IL10 efficacy *in vivo*

Long-term immunity suggests an activation of specific antitumor immune responses after treatment. To assess the contribution of different immune cells to treatment efficacy, $CD8^+$, $CD4^+$, or NK immune subsets were depleted from mice before treatment of subcutaneous DT6606 tumors with VVLΔTK-IL10 (Fig. 3B). Depletion of both $CD4^+$ and $CD8^+$ cells had a significantly detrimental effect on the efficacy of treatment, suggesting VVLΔTK-IL10 is acting via these immune subsets to eliminate the tumor. Surprisingly, given previous reports that IL10 can activate NK cells to mediate tumor clearance (17), depletion of NK cells in our experiment had no effect on treatment efficacy.

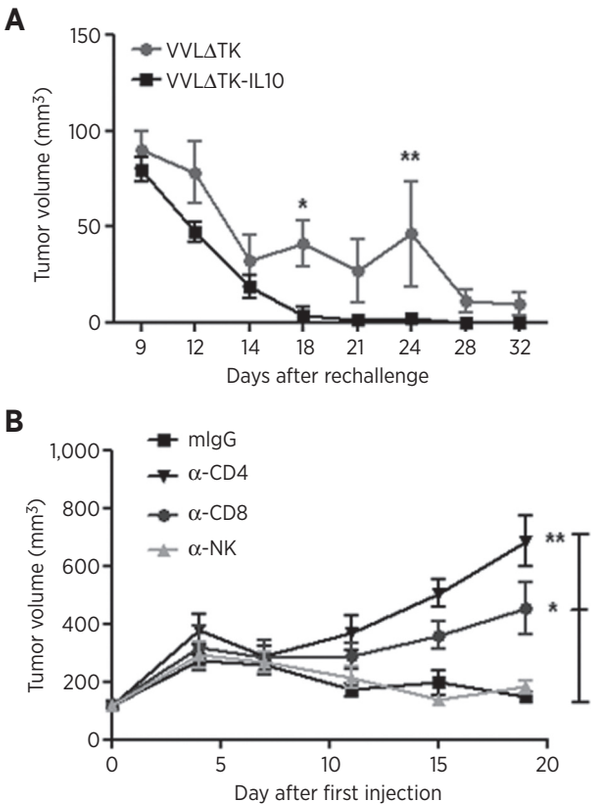

Figure 3.
Immune system involvement in the efficacy of VVLΔTK-IL10 *in vivo*. A, mice that had cleared tumors after i.t. treatment with VVLΔTK or VVLΔTK-IL10 during efficacy experiments were rechallenged 4 weeks later in the opposite flank with 4×10^6 DT6606 cells and tumor growth measured as previously. VVLΔTK $n = 3$, VVLΔTK-IL10 $n = 6$. Mean tumor size ± SEM are displayed and compared by one-way ANOVA with *post hoc* Bonferroni testing. *, $P < 0.05$; **, $P < 0.01$. B, DT6606 tumors were established in male C57/Black6 mice as described previously and 1 day before commencement of viral treatment, rat anti-mouse CD4, CD8, NK, or control monoclonal antibodies were injected i.p. Injections were continued twice weekly for the duration of the experiment and FACS analysis used to confirm depletion. Mean tumor size ± SEM are displayed and compared by one-way ANOVA with *post hoc* Bonferroni testing. *, $P < 0.05$; **, $P < 0.01$ ($n = 5$/group).

Tumor-associated activated T-cell and macrophage populations are altered after treatment with VVLΔTK-IL10 compared with VVLΔTK, which affects viral persistence

Given the involvement of T cells in VVLΔTK-IL10 treatment efficacy, tumor T-cell populations were analyzed in more detail. Pancreatic tumors of KPC transgenic mice treated as previously were harvested posttreatment and T-cell populations analyzed by IHC. We noted a significant increase in $CD3^+CD8^+$ infiltrate after treatment with both viruses compared with PBS (Supplementary Fig. S2) and a significant increase in $CD3^+CD8^+$ cells in VVLΔTK-IL10–treated animals at day 22 after infection compared with VVLΔTK–treated animals.

DT6606-subcutaneous tumors were also harvested for analysis of T-cell populations by FACS. In accordance with data obtained from KPC mice, we found a significant increase in tumor T-cell infiltrate after treatment with both viruses, with a significant increase in $CD8^+$ infiltrate into tumors of VVLΔTK-IL10–treated animals (Fig. 4A). However, most interesting was that in $CD4^+$ (data not shown) and, more significantly, $CD8^+$ populations (Fig. 4B), the proportion of activated ($CD45RB^{lo}/CD44^{hi}$) T cells in tumors treated with VVLΔTK was higher than those treated with VVLΔTK-IL10. IFNγ expression within VVLΔTK-IL10–treated tumors was also significantly reduced compared with VVLΔTK–treated tumors (Fig. 4C).

Tumor-associated macrophage populations were also assessed in KPC (Supplementary Fig. S3) and DT6606 tumor-bearing mice (Fig. 4D) after infection. We found that treatment with either virus increased macrophage infiltrate into tumors of KPC mice compared with PBS, but that treatment with VVLΔTK-IL10 resulted in a reduced macrophage tumor infiltrate compared with treatment with VVLΔTK. This result was mirrored in DT6606 tumor-bearing mice. Further assessment of macrophage activation status in the DT6606 subcutaneous model revealed that VVLΔTK-IL10 induces a downregulation of MHCII expression compared with VVLΔTK (Fig. 4E).

To assess the impact of these phenomena on viral persistence, viral DNA load in the tumors (6 mice/group/time point) was analyzed after i.t. treatment at days 8, 16, and 24 after infection using qPCR (Fig. 4F, i) and $TCID_{50}$ (Fig. 4F, ii). We found that by day 24, both viruses had been cleared from the tumor to the same extent, but at days 12 and 16, significantly more VVLΔTK-IL10 was recovered from tumors than VVLΔTK, indicating a delay in clearance of VVLΔTK-IL10 compared with VVLΔTK. These results were confirmed by IHC analysis of viral load in pancreatic tumors of KPC mice (Supplementary Fig. S4).

The splenic $CD4^+$ and $CD8^+$ cell populations are altered after treatment with VVLΔTK-IL10 compared with treatment with VVLΔTK

It is clear that VVLΔTK-IL10 treatment efficacy involves modulation of the immune system, thus splenic immune cell population dynamics in response to treatment were assessed in greater detail.

DT6606 tumor-bearing mice were treated as described and their spleens collected and assessed for presence of various immune cell subsets. No differences were found in splenic B cell ($B220^+$ cells), Treg ($CD4^+$, $CD25^{hi}$ cells), NK ($CD3^-$, $CD49b^+$ cells), or NKT populations ($CD3^+$, $CD49b^+$ cells) after treatment with either virus compared with PBS-treated animals (Supplementary Fig. S5).

Analysis of $CD4^+$ and $CD8^+$ populations revealed that frequencies of these populations were altered at early time points (Fig. 5A and D; Supplementary Fig. S6). At days 8 and 16, a significant increase in the frequency of total $CD8^+$ cells was seen after treatment with either virus; however, VVLΔTK-IL10 treatment resulted in fewer total $CD8^+$ cells than treatment with VVLΔTK (Fig. 5D). This phenomenon was also observed in the $CD4^+$ populations at day 16 after treatment (Fig. 5A).

Further examination revealed that after treatment with VVLΔTK-IL10 or VVLΔTK, T-cell populations shifted toward an effector/memory phenotype (Fig. 5B–F) at days 8 and 16. However, VVLΔTK-IL10 induced statistically fewer activated $CD4^+$ and $CD8^+$ T cells than VVLΔTK at days 8 and 16 after infection (Fig. 5B–F), as noted previously within the tumor.

VVLΔTK-IL10 treatment results in reduced antiviral immune responses compared with treatment with VVLΔTK, but an increased frequency of tumor-specific T cells

To clarify the proportions of virus-specific and tumor-specific splenic effector $CD8^+$ cells elicited after treatment with VVLΔTK and VVLΔTK-IL10, splenocytes from DT6606-OVA tumor-bearing animals were analyzed. For virus-specific T cells, an MHCI-specific pentamer against an immunogenic vaccinia virus antigen, B8R, was used (Fig. 6A and Supplementary Fig. S7A). As expected, viral treatment resulted in detection of B8R-specific $CD8^+$ cells in both treatment groups. However, VVLΔTK-treated animals had a significantly higher proportion of B8R-specific T cells than VVLΔTK-IL10–treated animals at all time points, suggesting a decreased virus-specific immune response after treatment with VVLΔTK-IL10, which could account for the fewer effector $CD8^+$ cells noted after VVLΔTK-IL10 treatment. We confirmed the decreased frequency of antivirus-specific T cells using an *in vitro* restimulation assay, in which IFNγ production from splenocytes in response to B8R peptide restimulation was measured (Fig. 6B). At all time points, significantly less IFNγ was detected from VVLΔTK-IL10 treatment groups compared with VVLΔTK treatment groups.

To assess T-cell reaction to tumor antigens, an MHCI OVA-specific pentamer was used in FACS staining (Fig. 6C and Supplementary Fig. S7B). At day 8, no differences in OVA-specific $CD8^+$ T cells was observed after treatment with either virus when compared with PBS; however, by day 16, VVLΔTK-IL10–treated animals showed an increase in production of OVA-specific antigens compared with VVLΔTK–treated animals. This result was reflected in restimulation assays (Fig. 6D).

Taken together, these results indicate that although VVLΔTK-IL10 treatment resulted in a reduction in antiviral T-cell production, the frequency of antitumor-specific $CD8^+$ T cells was comparable or even increased compared with VVLΔTK–treated mice.

Discussion

Efficacy of oncolytic virotherapy is dependent on both the oncolytic action of the virus itself and the effective stimulation of a local immune response to viral infection (36, 37). Oncolytic viruses may represent a method of achieving vaccination *in situ*, enabling the adaptive arm of the immune system to clear residual disease and provide long-term surveillance against relapse. To date, however, the use of oncolytic viruses alone has proved unsuccessful in clinical trials and this is likely due to their early clearance preventing their oncolytic effects and an effective immune-stimulating release of tumor-associated antigens (TAAs). Many viruses encode homologs of the cytokine IL10, generally considered immunosuppressive, to dampen the antiviral immune response and circumvent early viral clearance (11, 38). We aimed to adopt this natural strategy of viruses by arming vaccinia virus with IL10, which has been reported to be effective at prevention of vaccinia virus clearance (39). We hypothesized that prolonging viral persistence in the host would improve the antitumor efficacy by enhancing both the direct oncolytic effect and release of TAAs.

The pancreatic cancer subcutaneous tumor model we developed was based on the use of a DT6606 cell line, which was originally derived from the transgenic KPC spontaneous model of pancreatic cancer (29), and therefore accurately reflect the PDAC populations of cells within these mice. Previous study has demonstrated that these cancer cells resemble human PDAC in many respects, including their expression of oncogenic KrasG12D and the TAA mesothelin, and both spontaneous and subcutaneous tumors show similar histopathologic features such as the presence of FAP^+ stromal cells (40).

The long-held paradigm of IL10 function suggests it as an immunosuppressive cytokine, commonly investigated therapeutically in the context of treatment for inflammatory autoimmune conditions and allograft survival (41, 42). However, using these two different murine models of pancreatic cancer, we observed significantly enhanced therapeutic responses after treatment with our IL10-armed vaccinia virus compared with unarmed virus. In both models, low doses of the virus were sufficient to induce objective responses and in agreement with previous reports, no IL10-related toxicity was observed (43). Treatment also resulted in rejection of tumors after rechallenge, confirming the development of effective long-term immunity against tumor antigens. These results are consistent with those of others investigating the antitumor properties of IL10 in which systemic administration of recombinant protein or tumor cells transfected with IL10 induced tumor clearance and long-term memory responses in mice bearing sarcoma (16), melanoma (16, 44), colorectal cancers (16), breast cancers (45), and prostate cancers (20).

In vitro studies indicated that IL10 did not alter vaccinia virus replication or cytotoxicity and no effect on cell proliferation was observed. To determine other possible mechanisms for the superior efficacy associated with this virus, viral persistence within tumors was assessed. Although both IL10-armed and unarmed viruses were effectively cleared from animals, greater titers of VVLΔTK-IL10 were recovered at days 12 and 16 compared with VVLΔTK in both the transgenic and subcutaneous models of pancreatic cancer, suggesting that IL10 could significantly delay viral clearance.

Given previous reports of the ability of IL10 to stimulate NK cells (17) and as a cytotoxic T-cell differentiation factor (46), we examined reliance of our treatment on these immune subsets. Depletion of NK cells had no effect on treatment efficacy *in vivo* and we found no evidence of altered splenic or tumor (data not shown) NK populations after treatment with VVLΔTK-IL10. In contrast, depletion of $CD4^+$ and $CD8^+$ T-cell populations had a negative impact on treatment efficacy. It has previously been

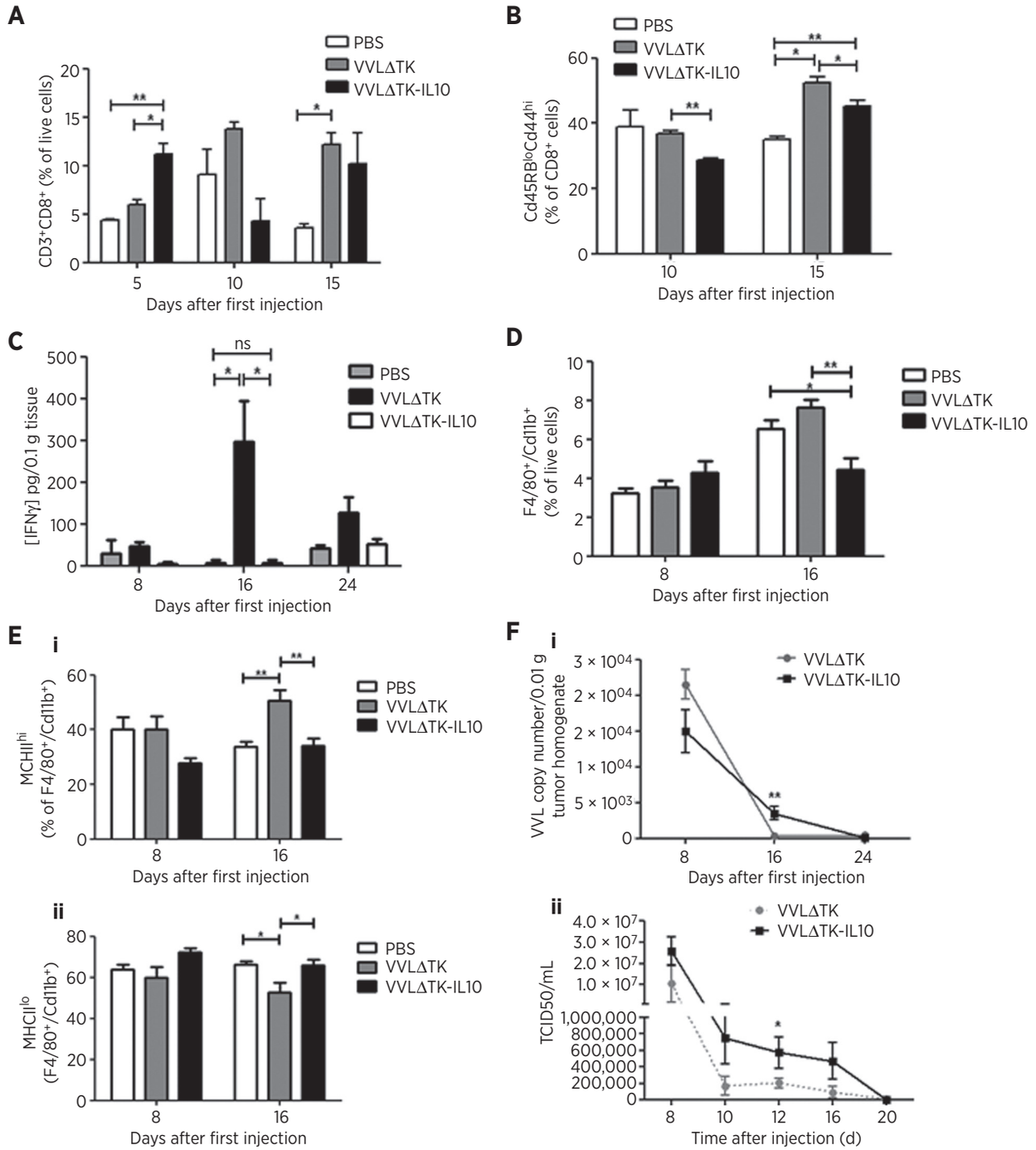

Figure 4.

Analysis of activated T cells, IFNγ expression, macrophage populations, and viral persistence in tumors. DT6606-OVA tumors were established and mice treated i.t. with VVLΔTK or VVLΔTK-IL10 following the same regimen as described for efficacy experiments. At days 10 and 15, tumors were harvested and analyzed using FACS analysis ($n = 3$/group). A, $CD8^+$ T cells as assessed by analysis of $CD3^+/CD8^+$ populations within $CD45^+$ populations. Mean populations ± SEM are displayed and compared by one-way ANOVA with *post hoc* Bonferroni testing. B, activated $CD8^+$ cells as assessed by analyzing $CD44RB^{lo}CD44^{hi}$ populations within the $CD8^+$ population. Mean populations ± SEM are displayed and compared by one-way ANOVA with *post hoc* Bonferroni testing. *, $P < 0.05$; **, $P < 0.01$. C, IFNγ expression within tumors was assessed by ELISA using tumor homogenates after treatment. Mean concentration/0.1 g tumor ± SEM are displayed and compared by one-way ANOVA with *post hoc* Bonferroni testing. D, DT6606-OVA tumors were established and mice were treated i.t. with VVLΔTK or VVLΔTK-IL10 following the same regimen as described for efficacy experiments. At days 8 and 16, tumors were harvested and analyzed for total macrophage populations using FACS analysis ($n = 3$/group). Macrophage activation status was also assessed using an MHCII marker, with MHCIIhi populations regarded as activated macrophages (E, i) and MHCIIlo populations regarded as naïve macrophages (E, ii). (*Continued on the following page.*)

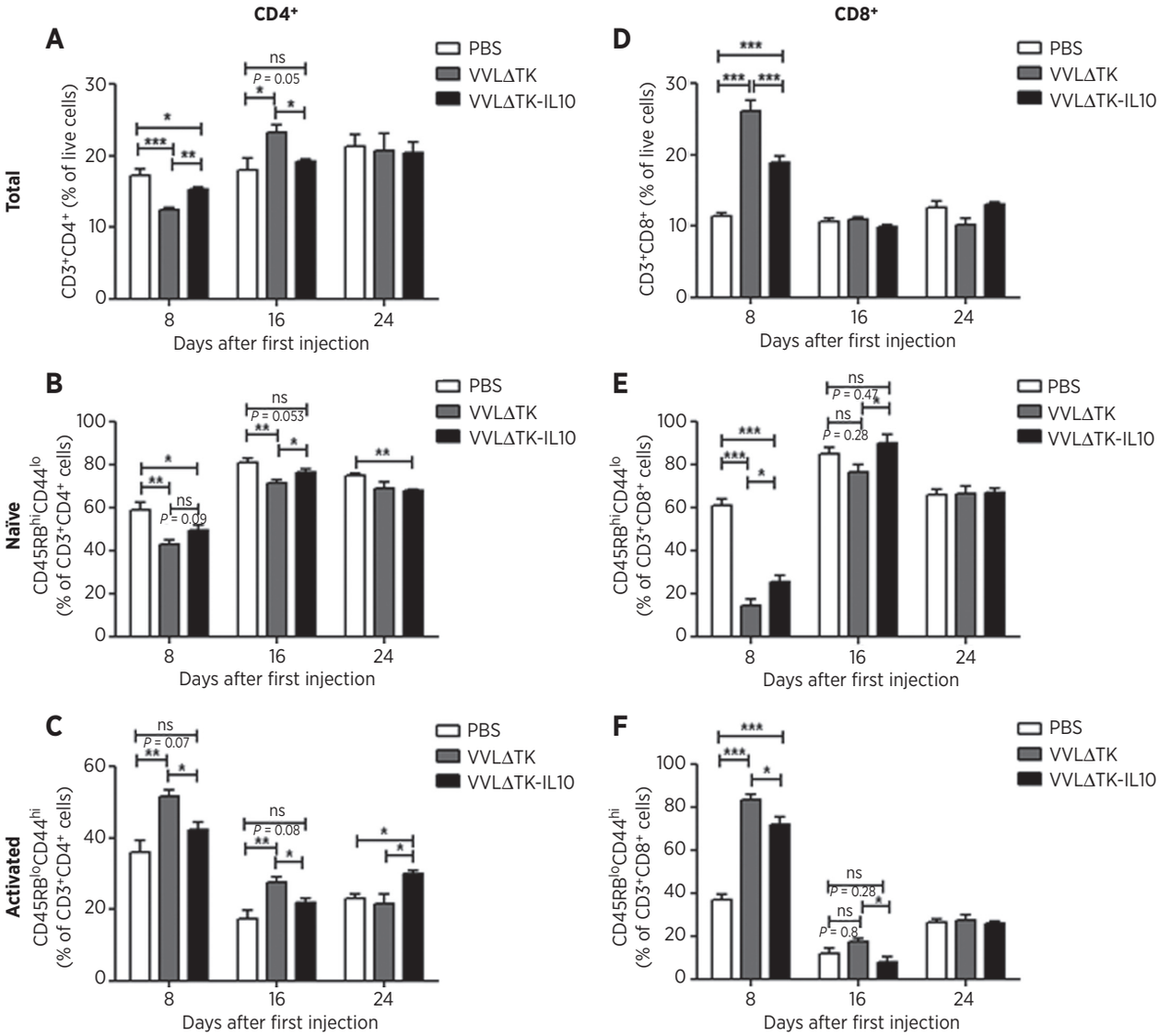

Figure 5.
Analysis of $CD4^+$ and $CD8^+$ populations and activation status in splenocytes of VVLΔTK-IL10- or VVLΔTK-treated mice. DT6606-OVA tumors were established and mice treated i.t. with VVLΔTK or VVLΔTK-IL10 following the same regimen as described for efficacy experiments. At days 8, 16, and 24, spleens were harvested and analyzed using FACS analysis ($n = 6$/group). A, CD4 populations as a percentage of live cells in splenocytes of treated mice assessed by gating on $CD3^+CD4^+$ populations. B, naïve CD4 cells as assessed by analyzing $CD44RB^{hi}CD44^{lo}$ populations within the $CD4^+$ population. C, activated CD4 cells as assessed by analyzing $CD44RB^{lo}CD44^{hi}$ populations within the $CD4^+$ population. D, CD8 populations in splenocytes of treated mice assessed by gating on $CD3^+CD8^+$ populations. E, naïve CD8 cells as assessed by analyzing $CD44RB^{hi}CD44^{lo}$ populations within the $CD8^+$ population. F, activated CD8 cells as assessed by analyzing $CD44RB^{lo}CD44^{hi}$ populations within the $CD8^+$ population. Mean populations ± SEM are displayed and compared by one-way ANOVA with *post hoc* Bonferroni testing. *, $P < 0.05$; **, $P < 0.01$; ***, $P < 0.001$. Representative FACS profiles with gating criteria are shown in Supplementary Fig. S6.

reported that progression from PanIN to PDAC is accompanied by progressive infiltration of T cells into the tumor in KPC transgenice mice (47, 48); however, no antitumor response is induced by this infiltrate. Our analysis of T-cell populations in spleens and tumors revealed that treatment with both unarmed and IL10-armed viruses induced a high level of adaptive immunity in mice

(*Continued.*) Mean populations ± SEM are displayed and compared by one-way ANOVA with *post hoc* Bonferroni testing. F, to assess viral persistence, DT6606 tumors were established and 18 mice per group treated i.t. with VVLΔTK or VVLΔTK-IL10 following the same regimen as described previously. At days 8, 16, and 24, tumors were harvested, viral DNA extracted, and viral DNA levels quantified in relation to a standard curve using qPCR (i). Mean vaccinia virus copy number ± SEM is displayed and analyzed at each time point using a Student unpaired *t* test. **, $P < 0.01$ ($n = 6$/group). Infectious virus recovered from homogenized tumors was also analyzed (ii). Mean viral replication ± SEM was determined by $TCID_{50}$ assay on CV1 cells. Statistical analysis was carried out using a Student unpaired *t* test at each time point. *, $P < 0.05$.

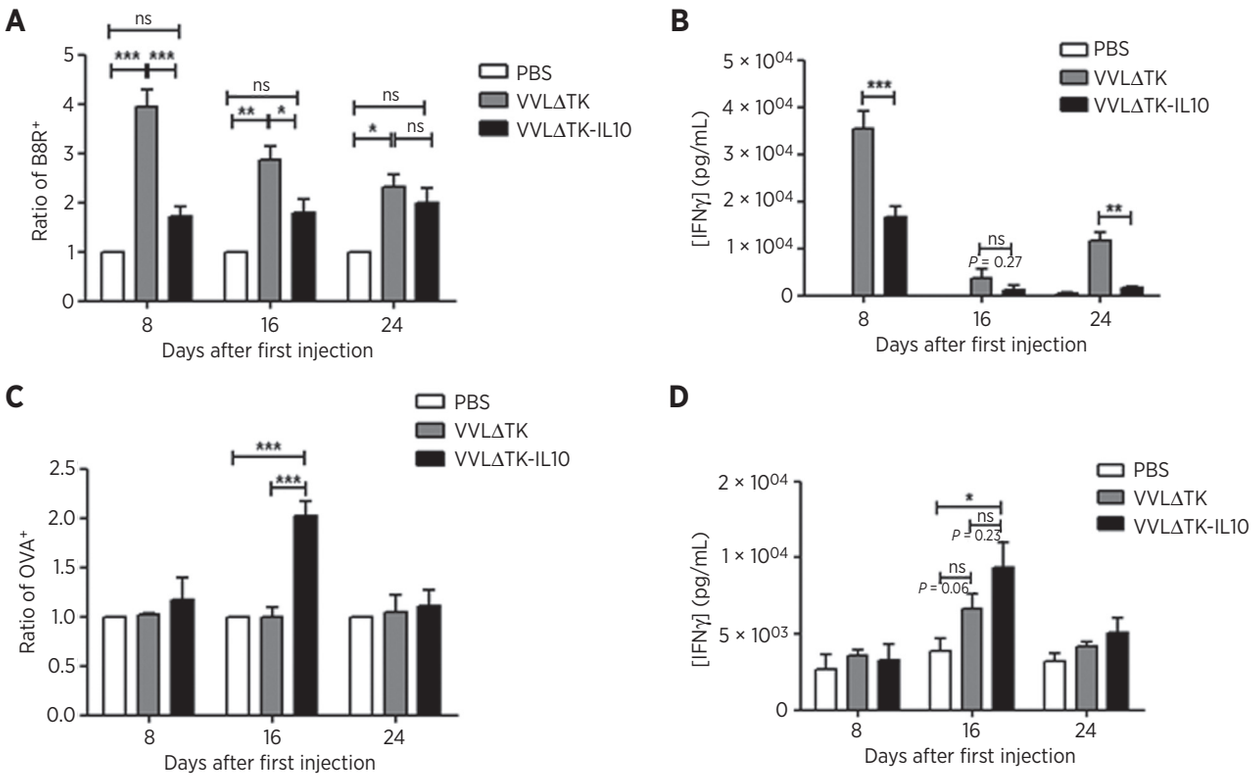

Figure 6.
Analysis of antiviral and antitumor specific CD8 cells in splenocytes of VVLΔTK-IL10- or VVLΔTK-treated mice. DT6606-OVA tumors were established and mice treated i.t. with VVLΔTK or VVLΔTK-IL10 following the same regimen as described for efficacy experiments. At days 8, 16, and 24, spleens were harvested for analysis ($n = 6$/group). A, harvested splenocytes were stained with anti-CD3, anti-CD8, and an H-2Kb–restricted, MHC class I anti-B8R pentamer (Proimmune). Mean $B8R^+CD8^+CD3^+$ cells from virus-treated animals are expressed relative to PBS-treated animals. Mean ratios ± SEM are shown for each group. B, splenocytes were incubated for 72 hours with a B8R peptide (Proimmune) and IFNγ production in response to stimulation measured by ELISA. Mean IFNγ levels ± SEM are shown. C, harvested splenocytes were stained with anti-CD3, anti-CD8, and an H-2Kb–restricted, MHC class I anti-OVA pentamer (Proimmune). Mean OVA^+ $CD8^+CD3^+$ cells from virus-treated animals are expressed relative to PBS-treated animals. Mean ratios ± SEM are shown for each group. D, splenocytes were incubated for 72 hours with mitomycin-treated DT6606-OVA cells and IFNγ production in response to stimulation measured by ELISA. Mean IFNγ levels ± SEM are shown. Statistical analysis was carried out using a Student unpaired *t* test. *, $P < 0.05$; **, $P < 0.01$; ***, $P < 0.001$. Representative FACS profiles are shown in Supplementary Fig. S7.

compared with untreated mice. However, an interesting finding was that the magnitude of the activated splenic $CD4^+$ and $CD8^+$ population response in VVLΔTK-IL10 treated mice was lower compared with the unarmed virus. This difference correlated with a reduction in virus-specific $CD8^+$ T cells and IFNγ recovery from tumors after VVLΔTK-IL10 treatment, which accounted for the delayed viral clearance from tumors. Interestingly, although VVLΔTK-IL10 treatment reduced antiviral $CD8^+$ populations, IL10 had no inhibitory effect on production of antitumor $CD8^+$ cells. Indeed, at day 16 after injection, an increase in anti-OVA $CD8^+$ cells was observed, which we postulate is a result of the increased oncolysis occurring with VVLΔTK-IL10 treatment, which improves TAA release.

These results suggest that IL10 improves the efficacy of OV by modulation of the early immune response to infection, resulting in dampening of antiviral, but not antitumor immunity. However, the mechanism by which IL10 elicits this alteration remains unclear. Our investigations revealed that local IL10 expression results in modification of the tumor macrophage population, which is highly sensitive to IL10 exposure (49). Numerous investigators have reported that IL10 can negatively regulate macrophages by (i) inhibiting their infiltration into tumors, and (ii) downregulating MHCII expression and suppressing production of proinflammatory cytokines and reactive nitrogen oxides (50). Although we found that VVLΔTK-IL10 treatment increased macrophage infiltrate into tumors in both the spontaneous and subcutaneous models of pancreatic cancer, we found that in accordance with previous data, VVLΔTK-IL10 treatment results in a significant downregulation of MHCII expression. Thus, it is feasible that in our model, tumor macrophages are responsible for viral antigen presentation to T cells and a reduction in macrophage activation by IL10 leads to reduced cross-priming of the antiviral immune response. A further consideration is that this model suggests distinct pathways of viral and tumor antigen presentation, which are the subject of ongoing investigation in our laboratory.

These findings demonstrate that IL10 armed vaccinia virus shows great promise as a novel therapeutic for pancreatic cancer, and that IL10 in combination with oncolytic virotherapy is clearly able to enhance tumor rejection through modulation of the innate and adaptive immune responses.

Disclosure of Potential Conflicts of Interest

No potential conflicts of interest were disclosed.

Authors' Contributions

Conception and design: L.S. Chard, I. Fodor, N.R. Lemoine, Y. Wang
Development of methodology: L.S. Chard, E. Maniati, P. Wang, F. Cao
Acquisition of data (provided animals, acquired and managed patients, provided facilities, etc.): L.S. Chard, E. Maniati, Z. Zhang, D. Gao, J. Wang, J. Ahmed, M. El Khouri, J. Hughes, B. Denes
Analysis and interpretation of data (e.g., statistical analysis, biostatistics, computational analysis): L.S. Chard, E. Maniati, J. Hughes, B. Denes, I. Fodor, Y. Wang
Writing, review, and/or revision of the manuscript: L.S. Chard, E. Maniati, J. Ahmed, J. Hughes, B. Denes, I. Fodor, N.R. Lemoine, Y. Wang
Administrative, technical, or material support (i.e., reporting or organizing data, constructing databases): L.S. Chard, J. Wang, S. Wang, X. Li, T. Hagemann, Y. Wang
Study supervision: I. Fodor, Y. Wang

Grant Support

This study was supported by The UK Charity Pancreatic Cancer Research Fund, the National Natural Science Foundation of China (81101608 and 81201792), Ministry of Sciences and Technology, China (2013DFG32080), the Henan Provincial Department of Science and Technology as well as the Department of Health, Henan Province, China (124200510018 and 104300510008).

The costs of publication of this article were defrayed in part by the payment of page charges. This article must therefore be hereby marked *advertisement* in accordance with 18 U.S.C. Section 1734 solely to indicate this fact.

Received February 24, 2014; revised September 20, 2014; accepted September 28, 2014; published OnlineFirst November 21, 2014.

References

1. Jemal A, Murray T, Ward E, Samuels A, Tiwari RC, Ghafoor A, et al. Cancer statistics, 2005. CA Cancer J Clin 2005;55:10–30.
2. Mulvihill S, Warren R, Venook A, Adler A, Randlev B, Heise C, et al. Safety and feasibility of injection with an E1B-55 kDa gene-deleted, replication-selective adenovirus (ONYX-015) into primary carcinomas of the pancreas: a phase I trial. Gene Ther 2001;8:308–15.
3. Hwang TH, Moon A, Burke J, Ribas A, Stephenson J, Breitbach CJ, et al. A mechanistic proof-of-concept clinical trial with JX-594, a targeted multi-mechanistic oncolytic poxvirus, in patients with metastatic melanoma. Mol Ther 2011;19:1913–22.
4. Breitbach CJ, Burke J, Jonker D, Stephenson J, Haas AR, Chow LQ, et al. Intravenous delivery of a multi-mechanistic cancer-targeted oncolytic poxvirus in humans. Nature 2011;477:99–102.
5. Yokoi K, Fidler IJ. Hypoxia increases resistance of human pancreatic cancer cells to apoptosis induced by gemcitabine. Clin Cancer Res 2004;10: 2299–306.
6. Hiley CT, Yuan M, Lemoine NR, Wang Y. Lister strain vaccinia virus, a potential therapeutic vector targeting hypoxic tumours. Gene Ther 2009; 17:281–7.
7. Fiorentino DF, Bond MW, Mosmann TR. Two types of mouse T helper cell. IV. Th2 clones secrete a factor that inhibits cytokine production by Th1 clones. J Exp Med 1989;170:2081–95.
8. Demangel C, Bertolino P, Britton WJ. Autocrine IL-10 impairs dendritic cell (DC)-derived immune responses to mycobacterial infection by suppressing DC trafficking to draining lymph nodes and local IL-12 production. Eur J Immunol 2002;32:994–1002.
9. Couper KN, Blount DG, Riley EM. IL-10: the master regulator of immunity to infection. J Immunol 2008;180:5771–7.
10. Wilson EB, Brooks DG. The role of IL-10 in regulating immunity to persistent viral infections. Curr Top Microbiol Immunol 2011;350:39–65.
11. Brooks DG, Trifilo MJ, Edelmann KH, Teyton L, McGavern DB, Oldstone MB. Interleukin-10 determines viral clearance or persistence *in vivo*. Nat Med 2006;12:1301–9.
12. von Bernstorff W, Voss M, Freichel S, Schmid A, Vogel I, Johnk C, et al. Systemic and local immunosuppression in pancreatic cancer patients. Clin Cancer Res 2001;7:925s–32s.
13. Bellone G, Turletti A, Artusio E, Mareschi K, Carbone A, Tibaudi D, et al. Tumor-associated transforming growth factor-beta and interleukin-10 contribute to a systemic Th2 immune phenotype in pancreatic carcinoma patients. Am J Pathol 1999;155:537–47.
14. Huang M, Wang J, Lee P, Sharma S, Mao JT, Meissner H, et al. Human non–small cell lung cancer cells express a type 2 cytokine pattern. Cancer Res 1995;55:3847–53.
15. Yigit R, Massuger LF, Figdor CG, Torensma R. Ovarian cancer creates a suppressive microenvironment to escape immune elimination. Gynecol Oncol 2010;117:366–72.
16. Berman RM, Suzuki T, Tahara H, Robbins PD, Narula SK, Lotze MT. Systemic administration of cellular IL-10 induces an effective, specific, and long-lived immune response against established tumors in mice. J Immunol 1996;157:231–8.
17. Zheng LM, Ojcius DM, Garaud F, Roth C, Maxwell E, Li Z, et al. Interleukin-10 inhibits tumor metastasis through an NK cell-dependent mechanism. J Exp Med 1996;184:579–84.
18. Toiyama Y, Miki C, Inoue Y, Minobe S, Urano H, Kusunoki M. Loss of tissue expression of interleukin-10 promotes the disease progression of colorectal carcinoma. Surg Today 2010;40:46–53.
19. Richter G, Kruger-Krasagakes S, Hein G, Huls C, Schmitt E, Diamantstein T, et al. Interleukin 10 transfected into Chinese hamster ovary cells prevents tumor growth and macrophage infiltration. Cancer Res 1993;53:4134–7.
20. Stearns ME, Wang M, Hu Y, Garcia FU, Rhim J. Interleukin 10 blocks matrix metalloproteinase-2 and membrane type 1-matrix metalloproteinase synthesis in primary human prostate tumor lines. Clin Cancer Res 2003;9:1191–9.
21. Rosenblum IY, Johnson RC, Schmahai TJ. Preclinical safety evaluation of recombinant human interleukin-10. Regul Toxicol Pharmacol 2002; 35:56–71.
22. Asadullah K, Sterry W, Stephanek K, Jasulaitis D, Leupold M, Audring H, et al. IL-10 is a key cytokine in psoriasis. Proof of principle by IL-10 therapy: a new therapeutic approach. J Clin Invest 1998;101:783–94.
23. Schreiber S, Fedorak RN, Nielsen OH, Wild G, Williams CN, Nikolaus S, et al. Safety and efficacy of recombinant human interleukin 10 in chronic active Crohn's disease. Crohn's Disease IL-10 Cooperative Study Group. Gastroenterology 2000;119:1461–72.
24. Nelson DR, Lauwers GY, Lau JY, Davis GL. Interleukin 10 treatment reduces fibrosis in patients with chronic hepatitis C: a pilot trial of interferon nonresponders. Gastroenterology 2000;118:655–60.
25. Kaufman HL, Rao JB, Irvine KR, Bronte V, Rosenberg SA, Restifo NP. Interleukin-10 enhances the therapeutic effectiveness of a recombinant poxvirus-based vaccine in an experimental murine tumor model. J Immunother 1999;22:489–96.
26. Emmerich J, Mumm JB, Chan IH, LaFace D, Truong H, McClanahan T, et al. IL-10 directly activates and expands tumor-resident CD8(+) T cells without *de novo* infiltration from secondary lymphoid organs. Cancer Res 2012;72:3570–81.
27. Kokura S, Yoshida N, Ishikawa T, Higashihara H, Sakamoto N, Takagi T, et al. Interleukin-10 plasmid DNA inhibits subcutaneous tumor growth of Colon 26 adenocarcinoma in mice. Cancer Lett 2005;218:171–9.
28. Tanaka F, Tominaga K, Shiota M, Ochi M, Kuwamura H, Tanigawa T, et al. Interleukin-10 gene transfer to peritoneal mesothelial cells suppresses peritoneal dissemination of gastric cancer cells due to a persistently high concentration in the peritoneal cavity. Cancer Gene Ther 2008;15:51–9.
29. Hingorani SR, Petricoin EF, Maitra A, Rajapakse V, King C, Jacobetz MA, et al. Preinvasive and invasive ductal pancreatic cancer and its early detection in the mouse. Cancer Cell 2003;4:437–50.
30. Denes B, Yu J, Fodor N, Takatsy Z, Fodor I, Langridge WH. Suppression of hyperglycemia in NOD mice after inoculation with recombinant vaccinia viruses. Mol Biotechnol 2006;34:317–27.
31. Tysome JR, Briat A, Alusi G, Cao F, Gao D, Yu J, et al. Lister strain of vaccinia virus armed with endostatin-angiostatin fusion gene as a novel therapeutic agent for human pancreatic cancer. Gene Ther 2009;16:1223–33.
32. Reed LJ, Muench H. A simple method of estimating fifty percent endpoints. Am J Hygiene 1938;27:493–7.
33. Workman P, Aboagye EO, Balkwill F, Balmain A, Bruder G, Chaplin DJ, et al. Guidelines for the welfare and use of animals in cancer research. Br J Cancer 2010;102:1555–77.
34. McCart JA, Ward JM, Lee J, Hu Y, Alexander HR, Libutti SK, et al. Systemic cancer therapy with a tumor-selective vaccinia virus mutant lacking

thymidine kinase and vaccinia growth factor genes. Cancer Res 2001;61: 8751–7.
35. Hingorani SR, Wang L, Multani AS, Combs C, Deramaudt TB, Hruban RH, et al. Trp53R172H and KrasG12D cooperate to promote chromosomal instability and widely metastatic pancreatic ductal adenocarcinoma in mice. Cancer Cell 2005;7:469–83.
36. Kaufman HL. The role of poxviruses in tumor immunotherapy. Surgery 2003;134:731–7.
37. Thorne SH. Immunotherapeutic potential of oncolytic vaccinia virus. Immunol Res 2011;50:286–93.
38. Fleming SB, McCaughan CA, Andrews AE, Nash AD, Mercer AA. A homolog of interleukin-10 is encoded by the poxvirus orf virus. J Virol 1997; 71:4857–61.
39. van Den Broek M, Bachmann MF, Kohler G, Barner M, Escher R, Zinkernagel R, et al. IL-4 and IL-10 antagonize IL-12-mediated protection against acute vaccinia virus infection with a limited role of IFN-gamma and nitric oxide synthetase 2. J Immunol 2000;164:371–8.
40. Kraman M, Bambrough PJ, Arnold JN, Roberts EW, Magiera L, Jones JO, et al. Suppression of antitumor immunity by stromal cells expressing fibroblast activation protein-alpha. Science 2010;330:827–30.
41. Whalen JD, Lechman EL, Carlos CA, Weiss K, Kovesdi I, Glorioso JC, et al. Adenoviral transfer of the viral IL-10 gene periarticularly to mouse paws suppresses development of collagen-induced arthritis in both injected and uninjected paws. J Immunol 1999;162:3625–32.
42. Shinozaki K, Yahata H, Tanji H, Sakaguchi T, Ito H, Dohi K. Allograft transduction of IL-10 prolongs survival following orthotopic liver transplantation. Gene Ther 1999;6:816–22.
43. Chernoff AE, Granowitz EV, Shapiro L, Vannier E, Lonnemann G, Angel JB, et al. A randomized, controlled trial of IL-10 in humans. Inhibition of inflammatory cytokine production and immune responses. J Immunol 1995;154:5492–9.
44. Huang S, Xie K, Bucana CD, Ullrich SE, Bar-Eli M. Interleukin 10 suppresses tumor growth and metastasis of human melanoma cells: potential inhibition of angiogenesis. Clin Cancer Res 1996;2:1969–79.
45. Kundu N, Beaty TL, Jackson MJ, Fulton AM. Antimetastatic and antitumor activities of interleukin 10 in a murine model of breast cancer. J Natl Cancer Inst 1996;88:536–41.
46. Chen WF, Zlotnik A. IL-10: a novel cytotoxic T cell differentiation factor. J Immunol 1991;147:528–34.
47. Clark CE, Hingorani SR, Mick R, Combs C, Tuveson DA, Vonderheide RH. Dynamics of the immune reaction to pancreatic cancer from inception to invasion. Cancer Res 2007;67:9518–27.
48. Mitchem JB, Brennan DJ, Knolhoff BL, Belt BA, Zhu Y, Sanford DE, et al. Targeting tumor-infiltrating macrophages decreases tumor-initiating cells, relieves immunosuppression, and improves chemotherapeutic responses. Cancer Res 2013;73:1128–41.
49. Bogdan C, Vodovotz Y, Nathan C. Macrophage deactivation by interleukin 10. J Exp Med 1991;174:1549–55.
50. de Waal Malefyt R, Haanen J, Spits H, Roncarolo MG, te Velde A, Figdor C, et al. Interleukin 10 (IL-10) and viral IL-10 strongly reduce antigen-specific human T cell proliferation by diminishing the antigen-presenting capacity of monocytes via downregulation of class II major histocompatibility complex expression. J Exp Med 1991;174: 915–24.